Response of a Supersonic Inlet to Downstream Perturbations

T. J. Bogar,* M. Sajben,† and J. C. Kroutil‡
McDonnell Douglas Corporation, St. Louis, Missouri

Experimental results are reported for flows in a ramp-type, external compression inlet with a large-aspect-ratio, rectangular cross section. The inlet was operated at a freestream Mach number of 1.84 with mechanically generated downstream perturbations. High-speed schlieren and time-dependent pressure measurements were employed extensively. In supercritical operation, pressure fluctuations throughout the inlet caused by the excitation varied linearly with the fluctuations at the exit station, even for large exit station amplitudes. In subcritical operation (buzz), the excitation interacted nonlinearly with the naturally present, highly periodic oscillations by either modifying the natural frequency, if the excitation was near a natural harmonic, or by having the excitation modulate the naturally occurring oscillation. In addition, the conditions at the two criticality boundaries were determined as a function of excitation amplitude and frequency.

Nomenclature

A = cross-sectional area
B,E = Fourier coefficients
f = frequency
h = channel height
j = running index
M = Mach number
$\tilde{M}$ = average Mach number defined by Eq. (2)
n = harmonic order
p = static pressure
P = rms value of local pressure normalized by rms value of exit amplitude
R = perfect gas constant
t = time
T = absolute temperature
u = x component of velocity vector
x = streamwise (horizontal) coordinate; $x=0$ at ramp lip, increasing downstream
y = transverse coordinate; $y=0$ locally at bottom wall, increasing upward
γ = ratio of specific heats
ρ = density

Subscripts

b = buzz
c = critical
e = exit station
ex = excitation
f = narrow-band filtered at excitation frequency
s = shock
v = choke point at exhaust; approximately coincides with rotor axis
o = throat
$1,2,\ldots$ = orders of harmonics
∞ = freestream

Superscripts

$(-)$ = time mean
$(\ )'$ = time-dependent part
$(\hat{\ })$ = root mean square (rms) of time-dependent part
$(\tilde{\ })$ = distance normalized by geometric throat height ($h_0 = 23.5$ mm), except in $\tilde{M}$

Received June 7, 1984; revision submitted Oct. 10, 1984.

*Scientist, McDonnell Douglas Research Laboratories. Senior Member AIAA.
†Staff Manager—McDonnell Douglas Fellow, McDonnell Douglas Research Laboratories. Associate Fellow AIAA.
‡Unit Chief—Laboratory, McDonnell Douglas Research Laboratories.

Introduction

FLOWS in supersonic inlets may exhibit large-scale, natural oscillations over a wide frequency range, with the most troublesome unsteadiness occurring below 300 Hz.[1-3] The magnitude of these oscillations varies with the inlet geometry and operating condition. At sufficiently low mass flows, the terminal shock may oscillate between an interior location and one outside the inlet. This oscillation generally occurs with frequencies below 100 Hz. During such "buzz"[4,5] large-amplitude, highly periodic pressure fluctuations occur within the inlet.

In ramjet propulsion systems, the inlet is connected to a combustor that may itself generate large-amplitude, self-sustained, highly periodic pressure oscillations.[6-9] The combustor oscillations alone are capable of unstarting an otherwise normally operating inlet. The potential exists for the inlet and combustor to form a resonant system.[10,11] Such coupling could create pressure oscillations within the propulsion system larger than those occuring in either component when operated individually.

This study investigated the response of a supersonic inlet to periodic pressure perturbations introduced at the downstream end over a wide range of operating conditions. These perturbations simulate the effects of combustor oscillation and also provide a periodic downstream boundary condition by which time-dependent computer codes attempting to calculate such flows may be validated. The time-mean behavior and naturally occurring unsteadiness of the inlet model used in this study have been reported previously.[12]

Of particular interest to this study was the determination of the conditions under which the terminal shock could be forced upstream past the cowl and ramp lips. As these transitions occur, the mass flow through the inlet decreases significantly and the thrust decreases accordingly.

Test Facility

Model

The inlet model (Fig. 1) is an external-compression, ramp-type inlet operated in a semifreejet mode in the exhaust of a supersonic nozzle. The geometric throat, which ocurs at the cowl lip, is 23.5 mm high. The ramp angle is 14.7 deg, which in conjunction with the freestream Mach number of 1.84 produces an attached weak oblique shock, yielding a ramp surface Mach number of 1.3. The inlet was designed so that

the oblique shock clears the cowl lip by 0.7 mm. The cowl lip is also exposed to the postshock Mach number of 1.3. Structural details and additional model dimensions are provided in Ref. 12.

An arbitrarily chosen exit station within the constant-area terminal segment ($\bar{x}_e = 21.91$) serves as the downstream boundary of the flowfield of interest and corresponds to a station just upstream of the fuel injection in a ramjet. The unsteady pressures measured at this location were used to normalize the unsteady pressures throughout the channel.

Supersonic flow is produced by a two-dimensional, convergent-divergent supersonic nozzle. The inlet is located in the core flow of the nozzle exit; the top and bottom nozzle wall boundary layers are removed through large slots above and below the ramp and cowl lips, respectively. Approximately 68% of the nozzle flow enters the inlet.

Exciter

Exit area modulation was accomplished by the exciter device shown in detail in Fig. 2. The principal components of the exciter are an elliptical cross-section rotor with the axis horizontal and normal to the flow, two flaps that can be tilted around the indicated hinge points, and two doors formed by the hinged end segment of the top and bottom walls. These components form a symmetric arrangement of four parallel flow passages, each shaped as a convergent-divergent channel and choked under all operating conditions. The doors and flaps are actuated remotely.

The total cross-sectional area at the choke point (the exhaust area) can be varied according to the relation

$$A_v = \bar{A}_v + A_v' \cos(2\pi f_{ex} t) \qquad (1)$$

where $\bar{A}_v$ is the time-mean value and A_v', f_{ex} are the amplitude and frequency of the time-dependent contribution, respectively. Equation (1) does not describe higher harmonics, which are of negligible amplitudes.

Variation of the three parameters on the right side of Eq. (1) is continous and noninteracting. The symmetry of the configuration represents an improvement over an asymmetric device used in earlier, similar experiments.[13,14]

The door positions determine the height of the two outer passages and thereby the time-mean area $\bar{A}_v$. The doors thus perform the control function of the conventional plug throttle commonly used in inlet testing.

The rotor modulates the heights of the two inner passages at twice the shaft frequency, with a constant amplitude of 3.18 mm, or 13.5% of the geometric throat height. The amplitude of the modulation is the same for both passages, but the relative phase between the two can be varied by using the flaps. In the flap position shown in Fig. 2a, the areas vary in phase; the minima and maxima coincide. If the flaps are set as shown in Fig. 2b, then the area variations are 180 deg out of phase and the occurrence of a minimum on one side is associated with a maximum on the other side. The sum of the two inner passage areas is then constant and the modulation amplitude A_v' is zero. Intermediate flap settings produce intermediate amplitudes.

An optical encoder mounted on the rotor shaft provides 360 pulses/rev for measuring the rotor speed and as a reference in the ensemble averaging of various signals.

Instrumentation

Fifteen channels of steady data were routinely recorded. Ten ports along the top wall and two along the bottom wall accommodate the sensors for fluctuating surface pressures. Similar ports, one each in the cowl and ramp slots, are used to detect passage of the terminal shock over the cowl and ramp lips. Miniature strain-gage-type transducers measure the unsteady pressures. The transducer signals were amplified, low-pass filtered at 10 kHz, and routed either for recording on FM tape or for further analog signal conditioning.

High-speed (5000 frames/s) schlieren motion pictures were made of the flowfield, with the field of view extending from the nozzle exit to $\bar{x} = 14.6$.

Two separate, removable 12-tube rakes were alternately installed at the model exit station to measure the vertical total-pressure profile. One rake could be traversing in the spanwise direction to determine two-dimensionality of the flowfield at the exit station. The other, fixed at the model midspan, was used in conjunction with the local time-mean wall static pressure to determine the Mach number profile needed to calculate $\tilde{M}_e$ [see Eq. (2)].

Test Parameters

The model displayed a one-parameter family of time-mean flows, obtained by adjusting the exit doors to control the

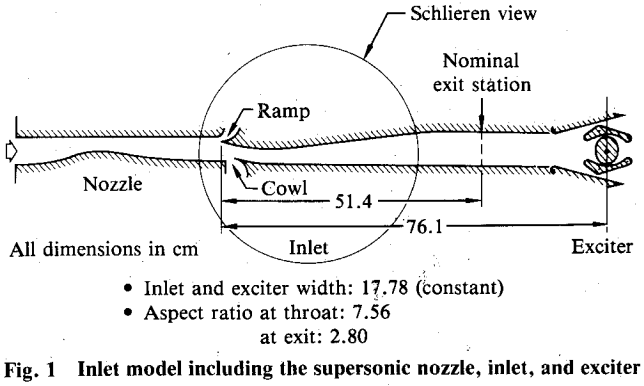

Fig. 1 Inlet model including the supersonic nozzle, inlet, and exciter components.

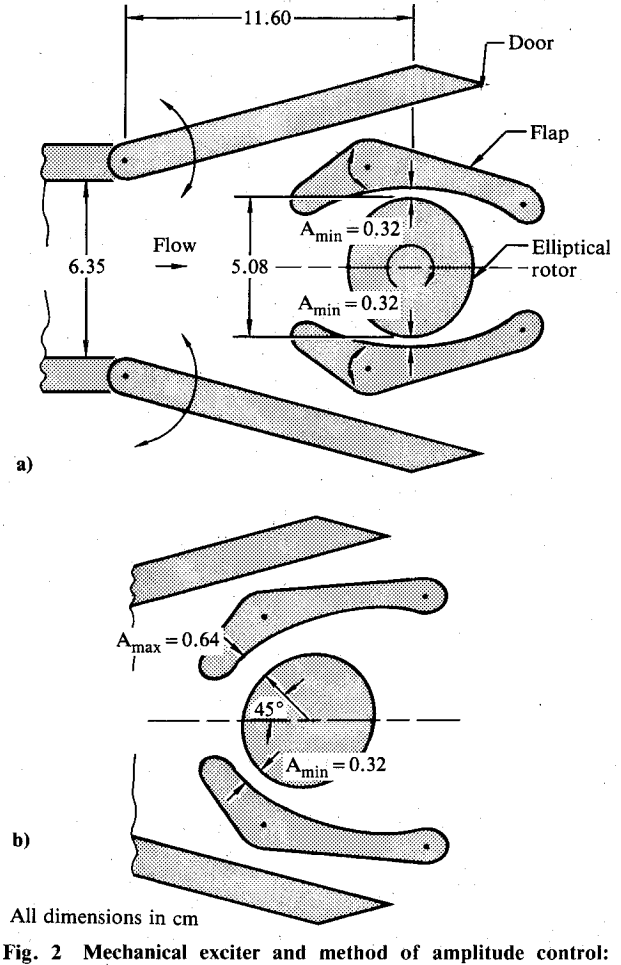

Fig. 2 Mechanical exciter and method of amplitude control: a) maximum amplitude and b) zero amplitude.

exhaust area $\bar{A}_v$. The exit station Mach number M_e was adopted as the principal test parameter. Since the flow at the exit station was nonuniform for the conditions of interest, an average Mach number $\tilde{M}_e$ was defined from midspan profiles of time-mean flow properties on the basis of energy considerations,

$$(\tilde{M}_e)^2 = \int_0^h \bar{\rho}(\bar{u})^3 \mathrm{d}y \Big/ \gamma R \int_0^h \bar{\rho}\bar{u}\bar{T}\mathrm{d}y. \qquad (2)$$

$\tilde{M}_e$ varied monotonically with $\bar{A}_v$ over the entire investigated range.

The excitation frequency f_{ex} was determined by the exit area modulation, which was twice the rotor shaft frequency. The intensity of excitation was measured by the exit pressure amplitude $\hat{p}_{ef}$, defined as the rms value of the narrow-band-filtered wall static pressure signal at the exit station top wall. The filter center frequency was slaved to the encoder output from the exiter; the filter bandwidth was 10 Hz.

The exit amplitude could be varied continuously by adjusting the exhaust area modulation amplitude controlled by positioning the exciter flaps. Five flap settings were selected to cover the available range of amplitude. In addition to zero and maximum modulation, three intermediate settings were selected so that at $\tilde{M}_e = 0.425$ and $f_{ex} = 350$ Hz, the respective $\hat{p}_{ef}$ values were 0.75, 0.5, and 0.25 times the maximum value. If $\tilde{M}_e$ and f_{ex} differed from these values, then the $\hat{p}_{ef}$ values obtained at the five flap settings generally did not form the above arithmetic sequence.

Terminology

The terminology used in this paper follows Ref. 12 and is briefly reviewed below.

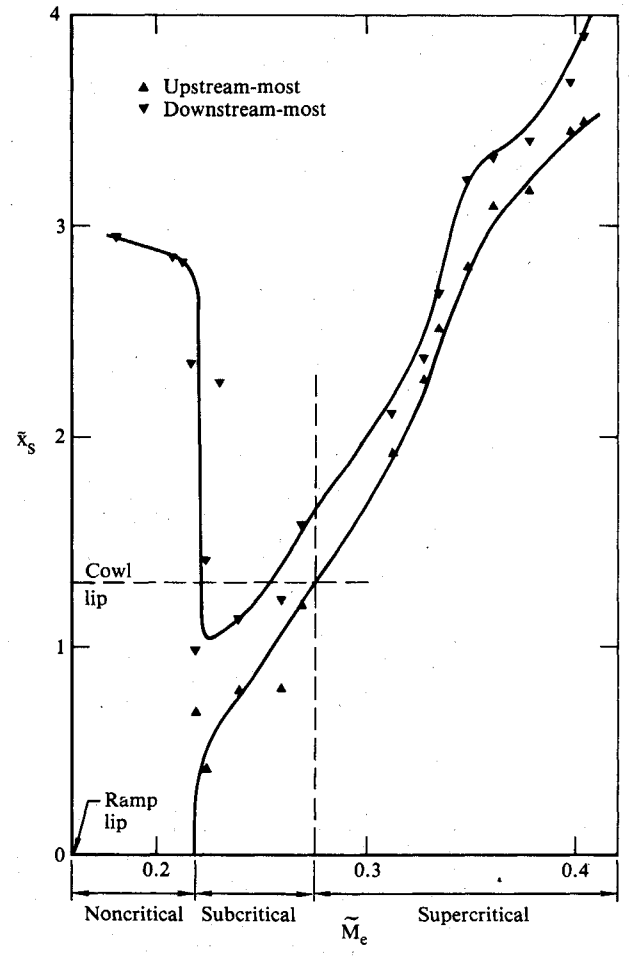

Fig. 3 Unexcited shock position extremes and criticality ranges.

Flow States

Classification of the instantaneous flowfields is based on the streamwise location of the terminal shock. The flow is said to be supercritical if the terminal shock is downstream of the geometric throat (cowl lip), subcritical if it is between the ramp and cowl lips, and noncritical if it is ahead of the ramp lip. Singular states occur if the shock is exactly at the throat (critical) or exactly at the ramp lip (incipient noncritical). Conventional usage considers noncritical states as part of the subcritical range; however, the distinction is necessary here because of the significant qualitative differences between subcritical and noncritical flows. Noncritical states were observed in the present experiment. They are expected (but not known) to occur in unbounded flight under conditions of low inlet mass flow that result in a large deflection of spilled flow.

Since natural oscillations are invariably present, any time-mean flow condition (fixed $\tilde{M}_e$) involves a range of instantaneous shock positions. Figure 3 illustrates the peak-to-peak ranges of shock position $\bar{x}_s$ found in the present model. The plot shows that some $\tilde{M}_e$ values may be associated with more than one type of criticality; for example, $\tilde{M}_e = 0.265$ is associated with a shock range that includes both super- and subcritical states. In such instances, the time-mean flow will be classified according to the state assumed by the terminal shock in its upstream-most position. At $\tilde{M}_e = 0.265$ the shock is subcritical in its upstream-most position and therefore the flow condition is called subcritical. Figure 3 illustrates the three time-mean criticality ranges in terms of $\tilde{M}_e$, in accordance with the present convention.

One might consider the time-mean shock position as a basis for defining time-mean criticality; however, important qualitative changes of behavior depend on the upstream-most shock position. Also, experimental determination of the upstream-most position is simpler, especially with solid sidewall inlet models that offer no optical access to the flow interior.

Oscillation Modes

The flow exhibited a variety of oscillations that were classified on the basis of the shock position ranges assumed during the motion.

Oscillations in which the instantaneous flow patterns remain in the same state of criticality are called purely super-, sub-, or noncritical. Oscillations involving two adjacent criticality states (Fig. 3, $0.255 < \tilde{M}_e < 0.276$) are called dual modes, with the additional qualifiers of super/sub (or sub/non) if the range needs to be described more precisely. Oscillations that encompass all three ranges of criticality (Fig. 3, $\tilde{M}_e < 0.22$) are labeled triple modes. These purely kinematic definitions of oscillation modes do not depend on the cause of the motion and are therefore applicable to both natural and forced oscillations.

The term "buzz" has been used in the literature to describe many types of inlet oscillations; therefore, it conveys little specific information other than that the oscillations are sustained spontaneously and the amplitudes vary from moderate to large. We use buzz to describe oscillations in which periodic changes of instantaneous criticality occur, including the dual and triple oscillation modes.

Criticality Boundaries

The set of flow conditions intermediate between two adjacent conditions of time-mean criticality are referred to as criticality boundaries. There are two such boundaries: the critical boundary (CB) corresponding to the limiting case between the super- and subcritical conditions and the incipient noncritical boundary (INB) separating the subcritical and noncritical conditions. The boundaries are defined in terms of the three time-mean parameters ($\tilde{M}_e$, f_{ex}, and $\hat{p}_{ef}$), which are themselves time-mean quantities.

Determining the criticality boundaries as a function of the time-mean operating condition is of interest because inlet

stability, mass flow through the inlet, and therefore system thrust all depend strongly on the time-mean criticality.

Unexcited Flows

Reference 12 describes in detail the behavior of the inlet model with steady exit boundary conditions. A brief summary is included here.

To operate the model, the doors were opened fully and the plenum was pressurized sufficiently (at least 520 kPa) to cause the initially formed shock system to be swallowed by the inlet. The doors were then adjusted to obtain the desired operating condition. The terminal shock moved upstream as the door was closed and could be located anywhere within the inlet. The shock could be driven completely into the nozzle by closing the doors sufficiently.

The present work covered all three ranges of criticality, from the noncritical ($\tilde{M}_e = 0.12$) to the moderately supercritical ($\tilde{M}_e = 0.42$) condition. In terms of a commonly used engineering definition of the degree of supercriticality $[(\bar{p}_{ec} - \bar{p}_e)/\bar{p}_{ec}]$, the maximum supercriticality was 18%.

For the range of flow conditions investigated, the flow was bilaterally symmetric, as measured by the traversing total-pressure rake, and possessed a reasonably two-dimensional central region.12 There was no clear evidence of flow separation in oil flow traces taken on either the top or bottom wall for $\tilde{M}e < 0.4$.

The inlet exhibited natural oscillations under all conditions. Figure 3 shows the upstream and downstream limits of the shock motion for a variety of criticality states. Purely supercritical and subcritical oscillations as well as a dual (super/sub) mode were found to exist. When the inlet was at the INB boundary, a minute additional closing of the doors caused the inlet to go into triple-mode buzz; noncritical conditions were invariably associated with full buzz. No purely noncritical and no sub/non dual modes were observed because of the proximity of the nozzle exit.

Supercritical oscillations were random, although at certain conditions the power spectral density distributions of the pressures indicated one or two broad peaks.

Oscillations in which the shock moves ahead of the cowl lip (even temporarily) were strictly periodic and displayed a spectrum composed of a set of sharp peaks extending up to six significant harmonics. The fundamental frequency was near 65 Hz. In all these cases, the vortex sheet generated by the bifurcation point (formed by the ramp and the terminal shocks) is a significant feature of the flow. The vortex sheet is ingested by the inlet and develops into a free shear layer that broadens to nearly half the channel height by $\tilde{x} \cong 16$.

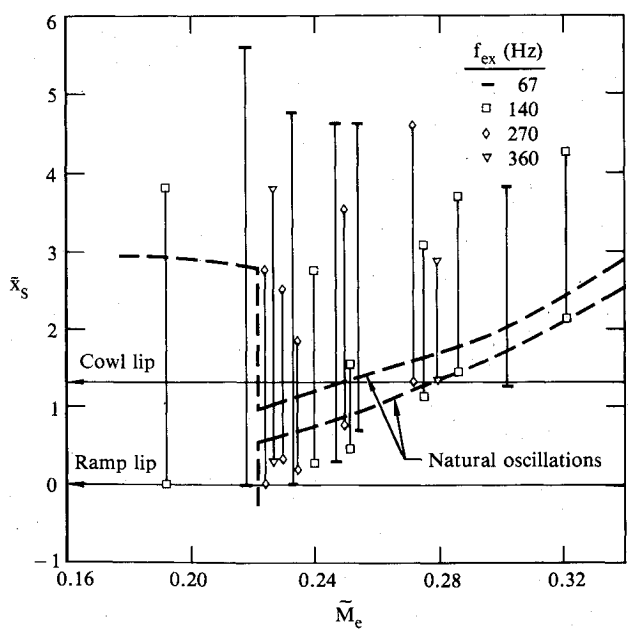

Fig. 4 Shock position ranges for forced oscillations, maximum flap setting.

Excited Flows

In a ramjet, downstream perturbations are introduced by combustion instabilities in the burner. The inlet and combustor oscillations are coupled; any perturbation of the flow entering the burner changes the combustion process, which in turn changes the inlet downstream boundary conditions and thereby the inlet flow. A theoretical description of this process requires the ability to predict both the response of the inlet to the downstream boundary conditions and the response of the combustor to the entering flow properties. The present work isolates and focuses on the inlet response.

The separation of the inlet from the combustor requires a somewhat arbitrary definition of a boundary surface separating the two. In the present experiment, the downstream boundary of the inlet was set arbitrarily at $\tilde{x}_e = 21.91$ (exit station). Fluctuations at the exit station were induced by mechanical modulation of the exhaust area. In a ramjet, combustion downstream of the exit area may be the cause of fluctuations. The two different inlet terminations produce identical flows in the inlet only if the exit station pressure histories are identical and if the inlet geometry and upstream boundary conditions are the same.

Operation of the exciter created periodic perturbation of all flow properties. The perturbations propagated upstream at the speed of sound with respect to the fluid and triggered complex responses from all points of the inlet that either propagated or were convected downstream. The perturbation pressure at the exit station is the sum of the original perturbation and the net result of all local responses; the two contributions cannot be separated in a steady oscillation. Thus, the measured exit station perturbations should not be thought of as inputs; they represent the input plus the response of the system. For this reason, $\hat{p}_{ef}$ is deliberately called the exit amplitude in preference to the possibly misleading term "excitation amplitude."

The time-dependent part of the measured flow quantities contained periodic contributions introduced by the exciter and random contributions from turbulent fluctuations. Interest was focused on the first harmonic of the periodic contribution, obtained by narrow-band filtering of the respective signals at the excitation frequency.

The parameters of the three-dimensional test matrix were the exit Mach number $\tilde{M}_e$, the excitation frequency f_{ex}, and the amplitude of the exit pressure $\hat{p}_{ef}$. This set is reasonably independent of facility-related effects, uniquely characterizes the flow, and is acceptable as input to theoretical considerations. The experimental control of these parameters, however, was neither direct nor independent. The excitation frequency was the only variable that could be set to any desired value independently of the other two parameters. In contrast, $\hat{p}_{ef}$ depended strongly on the setting of all three controls: rotor speed, doors, and flaps. $\tilde{M}_e$ depended primarily on the door setting, but rotor speed and flap setting also had non-negligible influences.

The mode of oscillation occurring at a specific flow condition could be determined reliably from high-speed films. Figure 4 illustrates the shock position ranges observed during forced oscillations as functions of $\tilde{M}_e$ superimposed on a plot of natural oscillation ranges. All forced oscillation data in the plot were taken with the flaps at the maximum setting. The amplitudes are greater by as much as an order of magnitude when excitation is present. One consequence of the large amplitudes is that purely subcritical oscillations were not found; only purely supercritical, sub/super dual, and triple buzz modes exist.

Figure 4 shows that excitation primarily extends the shock position range downstream at a given value of $\tilde{M}_e$, while the upstream-most shock location moves farther upstream by only a small amount. The time-mean shock position moves downstream by up to two throat heights; i.e., the presence of excitation has the same effect on the mean-flow condition as would an increase of the exhaust area. An alternative way of expressing this observation is to state that if the time-mean shock position is kept constant, then the imposition of forced oscillations reduces the associated $\tilde{M}_e$.

Supercritical Oscillations

In supercritical oscillations the shock always stayed downstream of the throat, the flow at the geometric throat was always steady, and the mass flow into the inlet was constant. These conditions combined to create a relatively simple type of motion.

Figure 5 illustrates the variation of the exit amplitude with the excitation frequency if the flap setting is held constant. The concurrent variation of the two principal parameters is evident. Results from (filtered) wall pressure transducers located at other interior points yield similar plots, but with differences in the locations and magnitudes of the minimum or maximum values. In light of the concurrent variation of f_{ex} and $\hat{p}_{ef}$, it is difficult to separate the frequency and amplitude effects.

The difficulties were greatly alleviated by the experimentally determined fact that the amplitudes of the wall pressure fluctuations at all interior locations vary linearly with the exit amplitude for any fixed frequency. All plots of $\hat{p}_f$ as a function of $\hat{p}_{ef}$ are straight lines described by equations of the form $\hat{p}_f = P(f)\,\hat{p}_{ef}$, where the dimensionless slope $P(f)$ depends on frequency only. The values of $P(f)$ were obtained by separate least-squares fits of straight lines to the data at each frequency. Normalizing this equation by $\bar{p}_e$ and dividing by $P(f)$ results in the representation given in Fig. 6, where the data taken at all frequencies collapse into a single straight line of slope unity, indicating that linearity holds at all frequencies. The quantity P depends only on f_{ex} and $\tilde{M}$; hence, its use for describing the response of the supercritically operated diffuser reduces the number of independent variables from three to two. Linearity failed only at locations that were intermittently passed over by the shock during its downstream excursions.

To the best of the authors' knowledge, the present results constitute the first experimental demonstration of the linearity of the response of such a complex flowfield to relatively large perturbations. Acoustic theories assume such linearity, but their basic assumptions usually require small-amplitude disturbances. In the present model, linear response was found at exit amplitudes up to 7.5% of the mean exit static pressure. The largest observed internal pressure amplitude was approximately 16% of the exit static pressure (at conditions other than those causing the previously mentioned 7.5% exit amplitude).

Figure 7 contains curves of normalized wall pressure as a function of frequency measured at $\tilde{x}=5.76$, downstream of the shock. The strong dependence of the inlet response on f_{ex} and $\tilde{M}_e$ is evident. Maximum response occurs at frequencies comparable to the first and second longitudinal acoustic modes (both ends closed).

Buzz with Excitation

Forced oscillations at sub- or noncritical mean flow conditions invariably involve periodic changes in criticality and are therefore classified as buzz. Dual- and triple-mode buzz both occurred (Fig. 4).

Triple-mode buzz displayed greater shock motion amplitudes than dual-mode buzz, but the differences between the two types of buzz with excitation were not as marked as without excitation. Excitation moved the mean shock position downstream, on occasion changing a triple mode into a dual mode by eliminating the noncritical portion of the oscillatory range. The similarities allow joint discussion of the two modes of forced buzz.

The case of $\tilde{M}_e=0.180$ with fixed maximum flap setting was selected for detailed study. At this condition, the unexcited flow displayed full buzz at 64 Hz. Attention was focused on pressure measurements at $\tilde{x}=4.15$, a location sufficiently downstream of the shock to remain subsonic at all times, yet sufficiently close to the shock to ensure similarity between the pressure and shock displacement spectra at low frequencies.

The power spectral density (PSD) distribution of the exit pressure in natural buzz is shown in Fig. 8a. The fluctuation is clearly dominated by periodic contributions consisting of several significant harmonics. Random contributions are negligible.

The exciter-generated perturbations could not be completely separated from the inlet response. However, if the terminal shock is weak, then the reflection from it is also weak[15] and the principal contribution to the measured exit pressure is expected to come from the upstream-moving wave initiated by the exciter. This situation is illustrated in the moderately supercritical case ($\tilde{M}_e=0.430$) of Fig. 8b. The

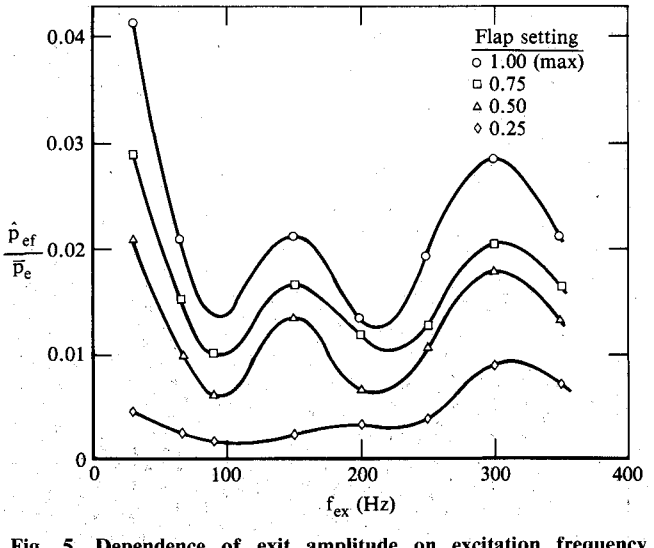

Fig. 5 Dependence of exit amplitude on excitation frequency ($\tilde{M}_e=0.420$, $\bar{p}_e\cong 390$ kPa).

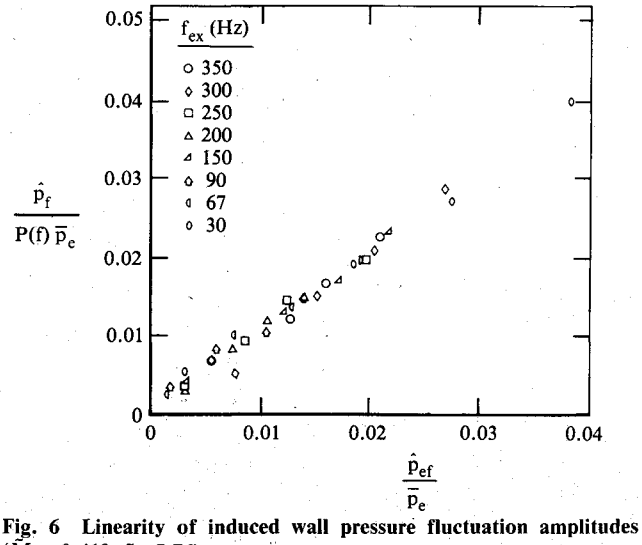

Fig. 6 Linearity of induced wall pressure fluctuation amplitudes ($\tilde{M}_e=0.410$, $\tilde{x}=5.76$).

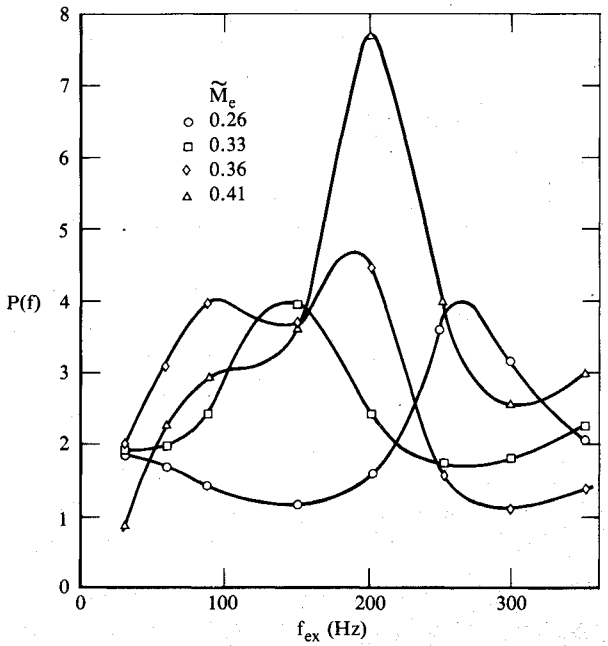

Fig. 7 Normalized wall pressure fluctuation amplitudes ($\tilde{x}=5.76$, maximum excitation).

PSD is dominated by a single sharp peak with insignificant higher harmonics, indicating that the excitation is essentially sinusoidal.

In this class of motions, the natural and forced contributions do not merely coexist, but interact with each other in various ways.

Modification of Buzz

If the excitation frequency was close to the first harmonic of the natural buzz frequency f_{b1}, then the resultant motion was similar to unexcited buzz; it merely occurred at the excitation frequency with larger amplitudes. The shock position range was displaced downstream, which in some cases changed the mode of oscillation from triple buzz to dual buzz. This modification of the natural frequency occurred over the range

$$0.5 \lesssim f_{ex}/f_{b1} \lesssim 1.3 \tag{3}$$

and is illustrated by the 38 and 76 Hz cases (Figs. 9a and 9b).

Modification also occurred when f_{ex} was near any higher harmonic of f_{b1}, although the frequency range for such coupling was increasingly narrower for higher harmonics. In such cases, the fundamental frequency was a submultiple of the excitation frequency,

$$f_1 = f_{ex}/n, \quad n=2, 3... \tag{4}$$

where f_1 was always close to, but not necessarily equal to, f_{b1}. Figure 9c illustrates a forced buzz spectrum for the $n=6$ case.

If modification occurs at the nth submultiple of f_{ex} then the amplitudes of the nth peak and of the fundamental both increase, while the other peaks remain largely unaffected. Furthermore, the greatest amplitude always occurs at the fundamental, regardless of which harmonic couples with the excitation frequency. This observation indicates a transfer of energy among harmonics, which is a typically nonlinear phenomenon.

Modulation of Buzz

If the excitation frequency is not close to the natural buzz frequency or one of its harmonics, then a different type of interaction takes place: the excitation modulates the buzz (for $f_{ex} < f_{b1}$) or the buzz modulates the excitation ($f_{b1} < f_{ex}$).

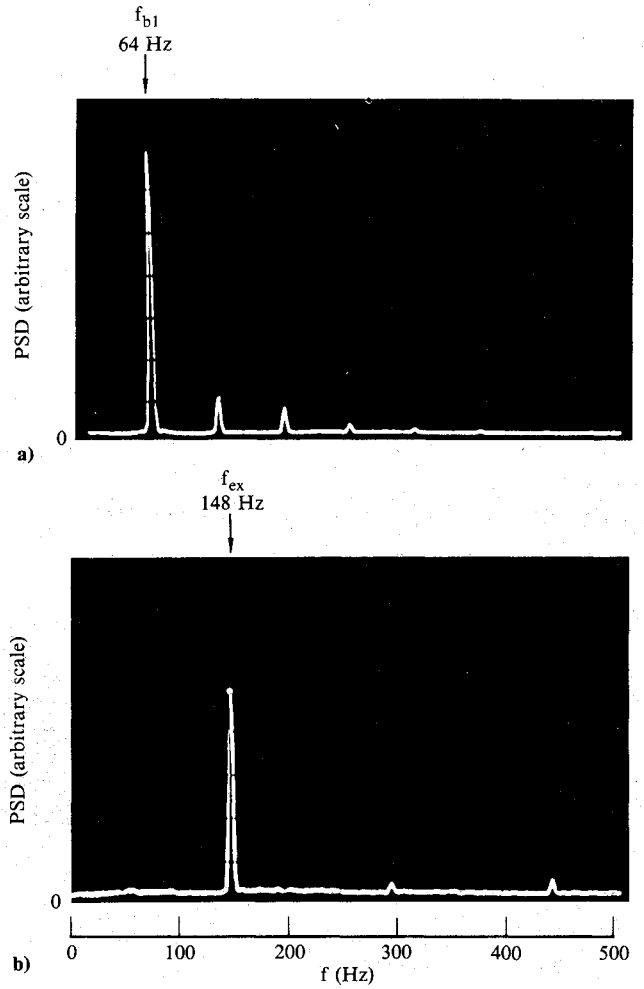

Fig. 8 Top-wall pressure PSD at $\tilde{x}=4.15$: a) $\tilde{M}_e=0.18$, unexcited, triple-mode buzz; b) $\tilde{M}_e=0.43$, supercritical, $f_{ex}=148$ Hz, maximum excitation.

Figure 10 shows the PSD for a case where f_{ex} is between f_{b3} and f_{b4}. The natural buzz pattern ($f_{bn}=nf_{b1}$, $n=1,2,3...$) appears along with the peak representing the excitation ($f=f_{ex}$). In addition, a number of new peaks appears, whose frequencies are found to be given precisely by

$$f_j = |f_{ex} \pm jf_{b1}|, \; j=1,2,3..., \tag{5}$$

the absolute values of the sums and differences of the excitation frequency and the buzz harmonics.

The additional frequencies can be explained as the result of amplitude modulation, which is, in effect, the multiplication of two waves having different frequencies. In this case, one wave is related to the excitation,

$$p_{ex}(t) = 1 + E_1 \cos(2\pi f_{ex} t) \tag{6}$$

and the other describes the buzz and its harmonics,

$$p_b(t) = \sum_{j=1}^{N} B_j \cos(2\pi j f_{b1} t) \tag{7}$$

where E_1 and B_j are constant coefficients and N the highest observed buzz harmonic ($N=6$). The product of the two series is another series with a general term of the form

$$\cos(2\pi f_{ex} t)\cos(2\pi j f_{b1} t) \tag{8}$$

which can be rewritten as

$$\tfrac{1}{2}\cos[2\pi(f_{ex} - jf_{b1})t] + \tfrac{1}{2}\cos[2\pi(f_{ex} + jf_{b1})t]. \tag{9}$$

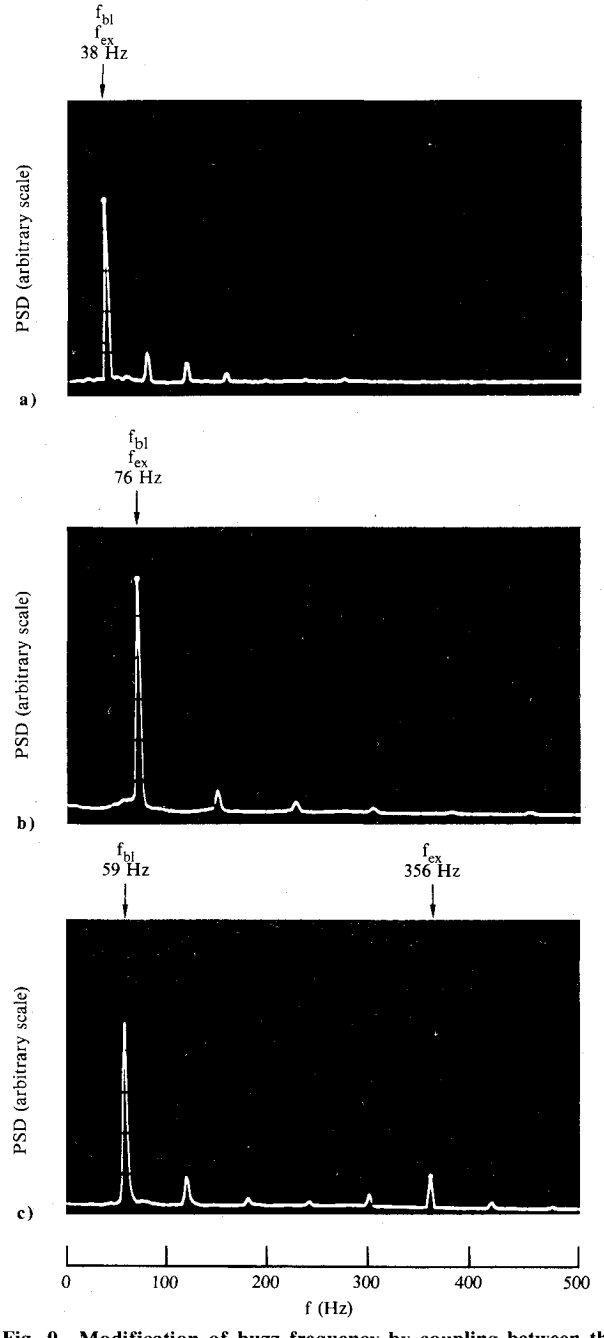

Fig. 9 Modification of buzz frequency by coupling between the excitation frequency and a buzz harmonic ($\tilde{M}_e = 0.180$, $\bar{x} = 4.15$, maximum excitation).

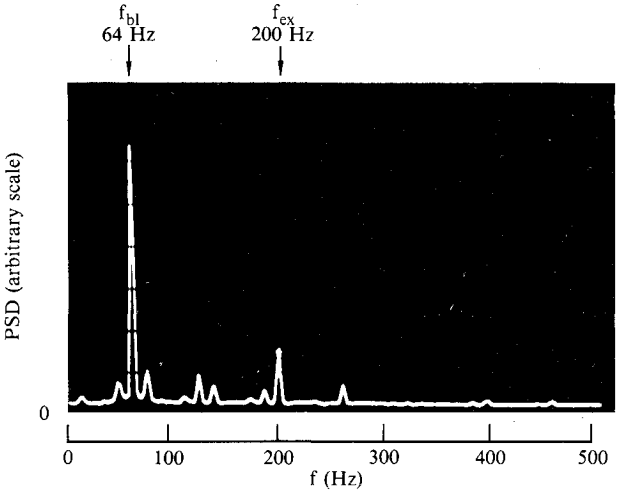

Fig. 10 Modulation of buzz by excitation ($\tilde{M}_e = 0.180$, $\bar{x} = 4.15$, maximum excitation).

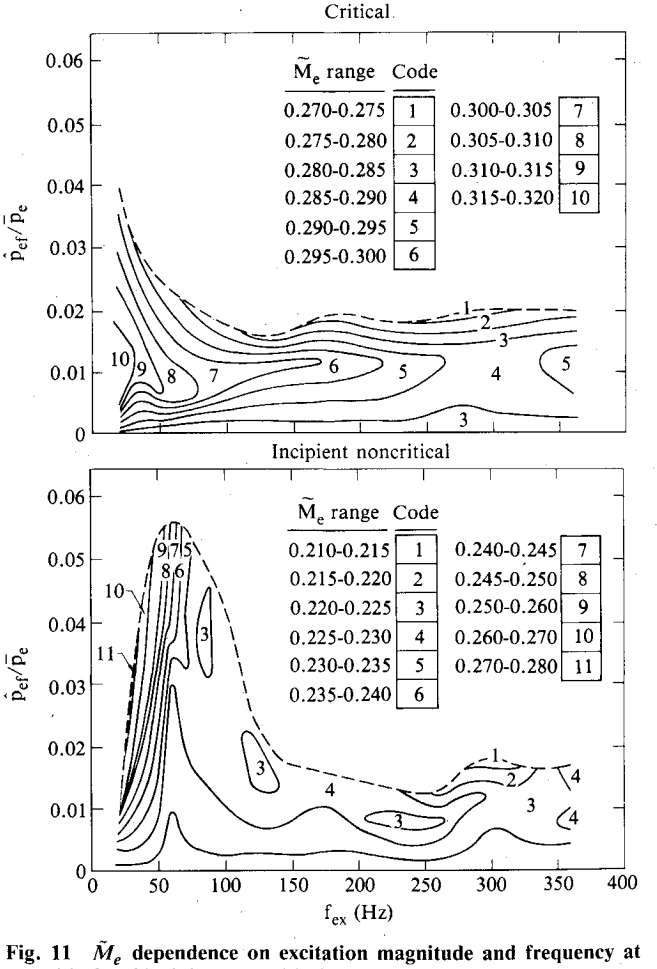

Fig. 11 $\tilde{M}_e$ dependence on excitation magnitude and frequency at the critical and incipient noncritical boundaries.

Linearity

The discussion of the previous sections indicates that both types of forced buzz are highly nonlinear phenomena. Linear amplitude response, which so conveniently simplified the description of purely supercritical oscillations, is not expected. Even if it were found, it would be accidental since no linear theory can describe the observed spectral transfer of energy and the observed amplitude modulation. Therefore, no attempt was made to establish the response as a function of excitation amplitude characteristics in this mode.

Criticality Boundaries

Passage of the terminal shock over the cowl or the ramp lips was detected by fast-response pressure transducers located on the outside of the cowl and ramp surfaces, i.e., on the downstream walls of the large suction slots separating the nozzle from the inlet. The boundaries were approached by gradually closing the doors, while keeping excitation frequency and flap position constant. The slot transducer signals were monitored visually during the process; the first appearance of perturbations indicated that the boundary had been reached. The door-closing process caused variations in the exit amplitude, so that the procedure resulted in a pair of $\hat{p}_{ef}$ and $\tilde{M}_e$ values associated with the criticality boundary for each flap setting and frequency. Since the flap setting is of no practical importance, it was eliminated by cross plotting the results to show $\tilde{M}_e$ values as a function of excitation intensity and

frequency, which are the operational parameters of concern (Fig. 11).

The bounary of the explored ($\hat{p}_{ef}$, f_{ex}) domain is irregular in each case, because of the maximum $\hat{p}_{ef}$ value obtainable by keeping the flaps at the maximum setting was a strong function of f_{ex}. The domain shape thus reflects experimental limitations only. The important feature is the $\tilde{M}_e$ values defining the boundaries. Higher $\tilde{M}_e$ indicates that a higher margin is required to prevent reaching the critical boundary (CB) or the incipient noncritical boundary (INB). Since the INB is also the boundary for the onset of triple-mode buzz, the INB is probably the more important of the two.

A dominant feature shared by the two boundaries is the rapid increase of $\tilde{M}_e$ as the frequencies decrease below ≈ 75 Hz. This frequency corresponds to the upper limit at which the excitation can couple to the buzz fundamental. Frequency dependence is weak above 75 Hz.

Dependence on exit amplitude is different for the two boundaries. For the CB, the $\tilde{M}_e$ value at the boundary peaks at $\hat{p}_{ef}/\bar{p}_e \cong 0.01$ regardless of frequency. This feature is puzzling since the expectation is that $\tilde{M}_e$ should increase monotonically with $\hat{p}_{ef}$: increasing excitation amplitudes should be associated with increasingly greater shock displacements and, since the upstream-most shock position tends to remain at the cowl or the ramp (see Fig. 4), the mean shock position should move downstream. In the absence of excitation, such a position is associated with stronger shocks, higher losses, and a higher exit Mach number. The experimental trend for $\hat{p}_{ef}/\bar{p}_e > 0.01$ is the opposite of this expectation, for reasons not understood.

The amplitude dependence of the INB differs considerably from that found in the CB (see Fig. 11). The INB displays little amplitude dependence above the buzz frequency, but below it, $\tilde{M}_e$ increases sharply with $\hat{p}_{ef}$. In addition to the frequency dependence already described, the low-frequency/high-amplitude combination is clearly the most likely cause for the inlet to reach the INB and the onset of triple-mode buzz.

Summary

The response of an external compression, $M_\infty = 1.84$ inlet to periodic downstream perturbations was explored experimentally over all ranges of criticality. The peak-to-peak amplitude of the exit station pressure fluctuations ranged up to 8% of the mean exit pressure at frequencies of 20-360 Hz.

In purely supercritical oscillations, the natural fluctuations are broadband and do not appear to couple strongly to the enforced periodic motion. The amplitudes of induced pressure fluctuations in the subsonic region (filtered at the excitation frequency) vary linearly with the excitation amplitude under all supercritical conditions. The response depends strongly on both frequency and mean flow conditions; and distinct frequencies of maximum sensitivity were found.

Subcritical and noncritical conditions are associated with natural oscillations at well-defined discrete frequencies, with minor contributions from random (turbulent) fluctuations. Downstream perturbation at frequencies close to the natural mode causes the natural mode to occur at the excitation frequency. If the natural and forcing frequencies are too far apart, then the observed waveforms of pressure as a function of time are precisely described as the product of the excitation waveform and the natural oscillation waveform, including the higher harmonics of the latter up to the sixth. Thus, the two oscillations modulate each other.

Criticality boundaries, defined as sets of flow conditions separating the supercritical/subcritical and the subcritical/noncritical flow condition ranges, were determined. The time-mean exit Mach number describing each boundary was virtually independent of frequency over 75 Hz and displayed sharp dependence on both amplitude and frequency below 75 Hz.

Acknowledgments

This work was sponsored by the Office of Naval Research under Contract N00014-80-C-0481.

References

[1] Sajben, M., Kroutil, J. C., and Chen, C. P., "Unsteady Transonic Flow in a Two-Dimensional Diffuser," *Unsteady Aerodynamics,* AGARD CP 227, 1977, pp. 13-1—13-14.

[2] Sajben, M. and Kroutil, J. C., "Effects of Initial Boundary-Layer Thickness on Transonic Diffuser Flows," *AIAA Journal,* Vol. 19, Nov. 1981, pp. 1386-1393.

[3] Bogar, T. J., Sajben, M., and Kroutil, J. C., "Characteristic Frequencies of Transonic Diffuser Flow Oscillations," *AIAA Journal,* Vol. 21, Sept. 1983, pp. 1232-1240.

[4] Ferri, A. and Nucci, L. M., "The Origin of Aerodynamic Instability of Supersonic Inlets at Supercritical Conditions," NACA RM L50K30, Jan. 1951.

[5] Fisher, S. A., Neale, M. C., and Brooks, A. J., "On the Sub-Critical Stability of Variable Ramp Intakes at Mach Numbers Around 2," National Gas Turbine Establishment (England), Rept. ARC-R/M-3711, Feb. 1970.

[6] Clark, W. H., "Static and Dynamic Performance Investigations of Side Dump Ramjet Combustors: Test Summary," Naval Weapons Center, China Lake, Calif., NWC TP6209, Dec. 1980.

[7] Clark, W. H., "Geometric Scale Effects on Combustion Instabilities in a Side Dump Liquid Fuel Ramjet," CPIA Pub. 366, Vol. I, 1982, pp. 595-604.

[8] Schadow, K. C., Crump, J. E., and Blomshield, F. S., "Combustion Instability in a Research Dump Combustor: Inlet Shock Oscillations," CPIA Pub. 347, Vol. III, 1981, pp. 341-356.

[9] Crump, J. E., Schadow, K. C., Blomshield, F. S., and Bicker, C. J., "Combination Instability in a Research Dump Combustor: Pressure Oscillations," CPIA Pub. 347, Vol. III, 1981, pp. 357-370.

[10] Rogers, T., "Ramjet Inlet/Combustor Pulsations Study," Naval Weapons Center, China Lake, Calif., NWC TP6053, Jan. 1980.

[11] Rogers, T., "Ramjet Inlet/Combustor Pulsation Analysis," Naval Weapons Center, China Lake, Calif., NWC TP6155, Feb. 1980.

[12] Sajben, M., Bogar, T. J., and Kroutil, J. C., "Experimental Study of Flows in a Two-Dimensional Inlet Model," AIAA Paper 83-0176, 1983 (also, *AIAA Journal,* to be published).

[13] Salmon, J. T., Bogar, T. J., and Sajben, M., "Laser Doppler Velocimeter Measurements in Unsteady, Separated, Transonic Diffuser Flows," *AIAA Journal,* Vol. 21, Dec. 1983, pp. 1690-1697.

[14] Sajben, M., Bogar, T. J., and Kroutil, J. C., "Forced Oscillation Experiments in Supercritical Diffuser Flows," *AIAA Journal,* Vol. 22, April 1983, pp. 465-474.

[15] Sajben, M. and Bogar, T. J., "Unsteady Transonic Flow in a Two-Dimensional Diffuser: Interpretation of Test Results," AFOSR-TR-0453, March 1982.